
ELSEVIER Applied Mathematics and Computation 116 (2000) 133–151

APPLIED MATHEMATICS AND COMPUTATION

www.elsevier.com/locate/amc

Retrieval of atmospheric NO_2, O_3, aerosol optical depth, effective radius and variance information from SAGE II multi-spectral extinction measurements

A.A. Lacis *, B.E. Carlson, J.E. Hansen

NASA Goddard Institute for Space Studies, 2880 Broadway, New York, NY 10025, USA

Abstract

The direct-beam spectral extinction of solar radiation contains information on atmospheric composition in a form that is essentially free from the data analysis complexities that often arise from multiple scattering. Ground based Multi-Filter Shadowband Radiometer (MFRSR) measurements provide such information for the vertical atmospheric column path, while solar occultation measurements from a satellite platform provide horizontal slices through the atmosphere. We describe application of a Multi-Spectral Atmospheric Column Extinction (MACE) analysis technique that we developed to analyze MFRSR data to occultation measurements made by Stratospheric Aerosol and Gas Experiment (SAGE II). For analysis, we select the 1985 Nevado del Ruiz volcanic eruption period to retrieve atmospheric profiles of ozone and NO_2, and changes in the stratospheric aerosol size and optical depth. The time evolution of volcanic aerosol serves as a passive tracer to study stratospheric dynamics, and changes in particle size put constraints on the sulfur chemistry modeling of volcanic aerosols.

Keywords: Remote sensing; SAGE II; Spectral retrieval; Aerosols; Aerosol size

* Corresponding author.

PII: S0096-3003(99)00200-3

1. Introduction

An early example of inferring stratospheric aerosol radiative properties from solar occultation measurements is the study by Hansen and Matsushima [1] where they measured the lunar eclipse brightness variations at several wavelengths in the visible following the large volcanic eruption of Mt. Agung in 1963. Here, beams of solar radiation that pass through the Earth's stratosphere and suffer extinction by volcanic aerosols, are refracted and mapped on the Lunar surface. The amount of extinction and its spectral dependence provide crude information on the volcanic aerosol optical depth and particle size. The basic methodology for lunar eclipse and occultation ray tracing through the Earth's atmosphere is described in detail by Link [2].

A similar strategy is used by the Stratospheric Aerosol and Gas Experiment (SAGE II) launched in October 1984 in a near-polar orbit [3] to measure directly the spectral extinction of sunlight during morning and sunset occultations. As the sun sets (or rises) multiple scans are made with a high-resolution (0.5 min of arc) field of view across the solar disk to measure simultaneously the vertical profile of atmospheric transmission at seven wavelengths (1.02, 0.94, 0.60, 0.525, 0.453, 0.448, and 0.385 μm, selected specifically to sample extinction by aerosols, water vapor, ozone, and NO_2).

The full retrieval procedure for SAGE II data analysis is effectively a 3-step process. The first step is to navigate and map the several thousand measurements that are taken during an occultation event to obtain slant-path data-averaged transmission profiles tabulated at 1-km height intervals. This involves the use of National Weather Service (NWS) pressure–temperature profiles at the geographic location of each occultation to calculate the atmospheric refraction and ray path, and to determine the tangent altitude for each observational point [4–6].

The second step is to convert the slant-path transmissions into vertical path spectral extinction profiles, followed then by the third step, which is to invert the spectral extinction at each altitude point to retrieve the local ozone, NO_2, aerosol and water vapor concentrations. In the current SAGE II retrieval algorithm [6], these steps are effectively reversed by first removing the Rayleigh extinction from the slant-path transmission, followed then by the absorbing species inversion and atmospheric profile determination. This approach imposes an artificial constraint on the aerosol spectral extinction dependence, in particular at the 0.60 μm channel that is used to retrieve ozone. This has been criticized by Steele and Turco [7] and by Fussen [8] as biasing the ozone retrieval, and they have suggested using a more rigorous spectral extinction interpolation scheme described earlier by Twomey [9]. Fussen also notes that with the current SAGE II retrieval scheme, potential error may be introduced by having to assume an altitude dependence for aerosol optical properties. To address these problems, Rusch et al. [10] developed a new SAGE II inversion

algorithm whereby they first perform a geometric slant-path matrix inversion followed by a species separation algorithm.

In our SAGE II analysis we adopt a similar approach and begin with the navigated and vertically mapped (step-1) slant-path extinction data product made available by the SAGE team, but we use a simpler slant-path geometric inversion than Rusch et al., followed by a brute-force least-squares simultaneous retrieval of ozone, NO_2, aerosol optical depth, effective radius and variance. Water vapor, which absorbs only within the 0.94 μm channel, is retrieved as a residual once the aerosol has been determined. Rigorous Mie scattering is used to specify aerosol spectral extinction. No other spectral interpolation is used.

2. Vertical path extinction determination

Altitude inversion of slant-path extinction profiles is accomplished by using a forward model to calculate the triangular matrix of the slant-to-vertical path extinction ratios. As shown schematically in Fig. 1, we assume a spherical shell model for the occultation geometry where the atmospheric constituents may vary linearly with height within each sub-layer, but have a horizontally uniform distribution. We begin by tabulating the number of molecules n_i (along a vertical path) per atmosphere layer at 1-km intervals, corresponding to the SAGE II slant-path extinctions S_i tabulated at the occulted ray tangent heights h_i. To evaluate $n(z)$, we use the same NWS pressure–temperature profiles that were used by the SAGE team to derive S_i. These are interpolated to 100 m

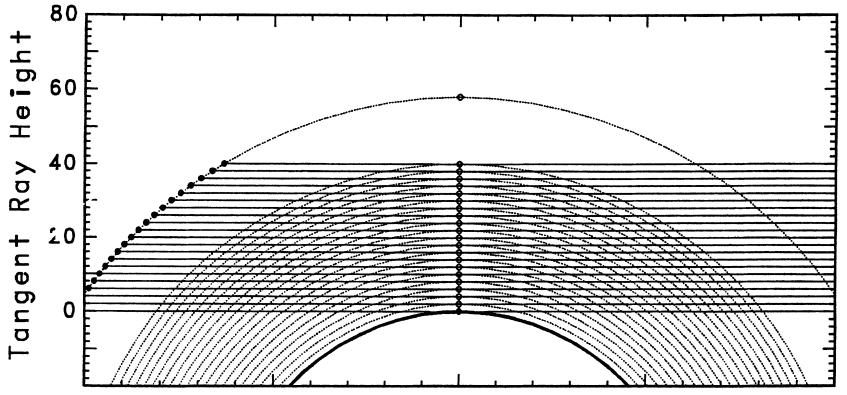

Fig. 1. Spherical shell model of occultation geometry for slant-path and vertical-path extinction. Open circles represent tangent ray heights and also refer the vertical-path extinction profile. The filled circles depict the spacecraft position during observation of occulted rays that contain the atmospheric slant-path extinction information. The geometric scaling is schematic in nature.

subintervals (assuming for this the ideal gas law and hydrostatic equilibrium) such that $n(z) = A + Bz$ provides a sensibly accurate representation for the vertical change in gaseous number density. We define also the cumulative column molecular path to the Top of the Atmosphere (TOA) above the height levels h_i

$$N_{ij} = \sum_{j=i}^{N} n_j, \tag{1}$$

where $N \approx 100$ represents the effective TOA.

Since the ray paths through the atmosphere have already been navigated to obtain the SAGE II slant-path data product, we need only to determine the slant-path molecular extinction using the integral representation for the curved ray path (due to refraction) through the atmosphere as given by Link [2]

$$m_i = 2 \int_{z_i}^{z_{i+1}} \frac{n(z) z \, \mathrm{d}z}{\sqrt{z^2 - u^2 z_i^2}}, \tag{2}$$

where $u = \mu_i/\mu$ is the refractive index of air ratioed relative to the reference level z_i, and where $z = h + R_0$ is the absolute ray height and R_0 is the radius of the Earth. The refractive index for dry air (including corrections for pressure and temperature dependence) is taken directly from Allen [11]. Within the specified subintervals, the refractive index ratio is expressed as a linear function of height, $u(z) = \alpha + \beta z$. This permits piecewise analytic evaluation of the above integrals. Thus, analogous to (1), we can define the slant-path column molecular path to the TOA above the tangent ray height levels h_i

$$M_{ij} = \sum_{j=i}^{N} m_j. \tag{3}$$

The average Rayleigh scattering cross-section per air molecule, including the correction for depolarization due to molecular anisotropy, is given by Hansen and Travis [12]

$$\sigma_\lambda = \frac{3\pi^3}{3} \frac{(\mu^2 - 1)^2}{\lambda^4 N^2} \frac{6 + 3\delta}{6 + 7\delta}, \tag{4}$$

where λ is the wavelength in microns, N is the number of air molecules per unit volume, and $\delta = 0.0279$ is the depolarization correction parameter for dry air [13]. Since the Rayleigh cross-section is effectively constant with height, varying only by a few part in the fourth decimal, the slant-path to vertical path ratios for both Rayleigh extinction as well as for total extinction are given by $r_k = m_k/n_k$ and by $R_{ij} = M_{ij}/N_{ij}$ for individual layer and column cases, respectively. (We include the small contributions due both to Rayleigh pressure–temperature dependence and to refractive index spectral dependence.)

Within this framework, the SAGE II slant-path extinctions can be written as

$$S_i = \sum_{k=i}^{N} s_k = \sum_{k=i}^{N} r_k v_k, \tag{5}$$

where v_k are the individual atmospheric layer vertical-path total extinctions. We determine the v_k by unraveling (5) from the top. Thus,

$$v_N = S_N / R_{N,N}, \tag{6a}$$

$$v_{N-1} = (S_{N-1} - R_{N-1,N} v_N)/r_{N-1,N-1}, \tag{6b}$$

$$v_{N-2} = (S_{N-2} - r_{N-2,N-1} v_{N-1} - R_{N-2,N} v_N)/r_{N-2,N-2}, \tag{6c}$$

$$v_{N-j} = \left(S_{N-j} - \sum_{k=1}^{N-j} r_{k,k+1} v_{k+1} - R_{N-j,N} v_N \right) \Big/ r_{N-j,N-j}, \tag{6d}$$

where S_N in (6a) is the slant-path extinction at the highest tabulated altitude of the slant-path SAGE II data product; v_N is the column extinction above this level, and $R_{N,N}$ the corresponding slant-path to vertical-path extinction ratio. The v_N below this point are given at 1-km intervals.

Since both the slant-path and vertical-path Rayleigh extinction contributions are known with high precision (given the specified pressure–temperature profile), we can thus subtract the Rayleigh extinction from v_N to yield the non-Rayleigh vertical-path extinction at each filter wavelength in the form

$$\tau_{in} = v_{in} - \sigma_{\lambda} n_i. \tag{7}$$

In the above, $\sigma_{\lambda} n_i$ is Rayleigh extinction optical depth in the ith layer, and the additional index n has been added to account for the 7 SAGE II spectral channels. Examples of SAGE II slant-path extinction profiles are shown in Fig. 2a, while in Fig. 2b we show the corresponding geometry-inverted profiles for the vertical-path non-Rayleigh extinction. This serves as the basic input to the step-3 MACE analysis part of the data retrieval procedure.

It is apparent from the tabulated slant-path extinctions that at high altitudes poor signal-to-noise, upper atmosphere turbulence and inaccuracies in assumed pressure–temperature profile hinder the accurate navigation of occulted light rays resulting in noisy and even negative extinctions above 60 km. Obviously, these deficiencies do carry over to the vertical-path extinctions. However, by good fortune, these errors do not grow and accumulate, but tend rather to dissipate as they get averaged out on the way down and are swamped by the increasingly larger extinctions of the lower altitudes. Accordingly, vertical-path extinctions appear to be generally robust below 40 km, with no significant assumptions or approximations having been made in this step of the retrieval analysis. We agree with Rusch et al. [10] that it makes good sense to perform the geometric inversion first, followed then by the species inversions at

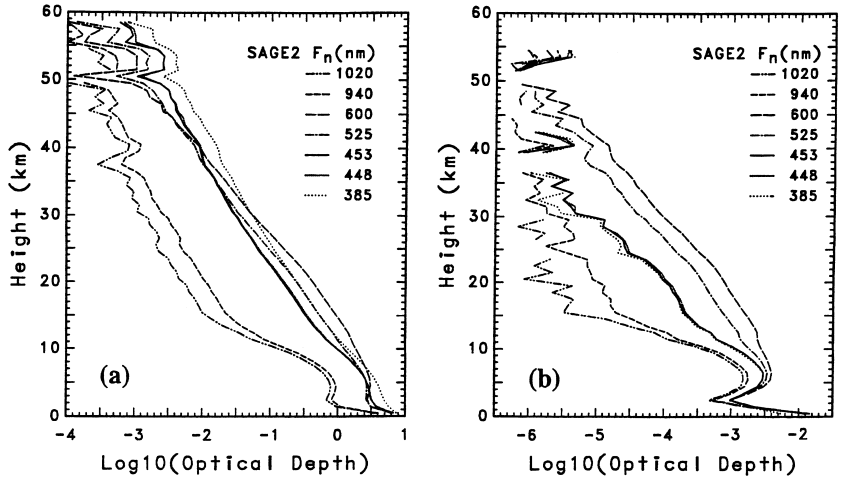

Fig. 2. SAGE II atmospheric extinction profiles at tangent ray altitudes defining (a) the observed slant-path extinction, and (b) the inverted vertical-path extinction.

each specified altitude, which can now be done independently of neighboring altitude influence.

3. MACE retrieval algorithm

The relevant atmospheric constituents that contribute extinction at SAGE II wavelengths are: Rayleigh scattering (which has already been subtracted out), ozone, NO_2, aerosol, H_2O (affecting only the 940 nm channel), and clouds (which when present tend to saturate in all channels which effectively terminates the occultation data at the cloud-top level). From here on, the (step-3) procedure to retrieve the contributing species amounts is basically identical to the Multi-spectral Atmospheric Column Extinction (MACE) analysis [14] procedure that we have used in previous analysis of ground-based Multi-Filter Shadowband Radiometer (MFRSR) extinction measurements. For numerical convenience, we can write the SAGE II vertical-path extinction (7) in matrix form as

$$\tau_{in} = \delta_{ik} a_{kn}, \tag{8}$$

where τ_{in} is a 7-column matrix with n referencing the seven SAGE II channels, and i denoting the ith altitude. Formally, the contributing absorber amounts δ_{ik} can be represented as a 5-column matrix depicting the height profile variations in aerosol optical depth, NO_2, O_3, H_2O, and cloud amount. However, cloud optical depth generally is either zero or saturated, and since water vapor

absorbs only in the 940 nm channel, it follows that its absorber amount will always be the residual non-aerosol optical depth within that channel. Thus aerosol, NO_2, and O_3, are effectively the principal unknown absorbers, their amounts constrained by their spectral extinction sampled at the six SAGE II wavelengths.

Absorption coefficients are weighted by the solar spectrum and the respective filter functions, to define the filter/absorber matrix elements

$$a_{kn} = \frac{\int_0^\infty K_k(\lambda)F_n(\lambda)S(\lambda)\,\mathrm{d}\lambda}{\int_0^\infty F_n(\lambda)S(\lambda)\,\mathrm{d}\lambda}. \tag{9}$$

The SAGE II filter response functions, F_n, are shown relative to the solar flux at the TOA in Fig. 3a, and relative to NO_2 and O_3 spectral absorption coefficients in Fig. 3b. Accurate measurements of NO_2 absorption have been tabulated at high spectral resolution over a broad range of atmospheric temperatures [15–17]. For ozone, we use absorption data compiled by E.P. Shettle of NRL [Private communication, 1997]. Temperature corrections, which may differ substantially at different wavelengths, are applied to the NO_2 and O_3 absorption coefficients at each level of the atmosphere.

For aerosols, their extinction spectral dependence is fully defined and strongly constrained by Mie scattering theory, given the aerosol refractive index and particle size distribution. For radiative transfer purposes, it is convenient to use the area weighted effective radius, r_{eff}, and effective variance, v_{eff}, to characterize aerosol size since these parameters tend not to be sensitive to the detailed form of the aerosol size distribution [12]. As shown in Fig. 4a, for

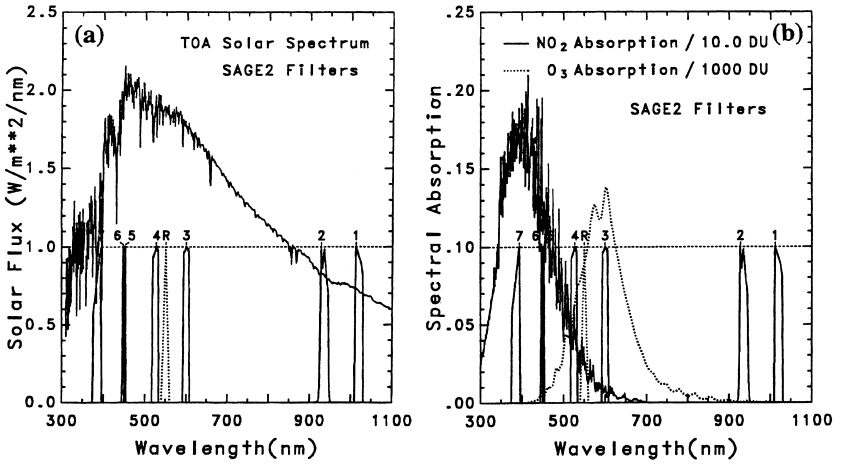

Fig. 3. SAGE II filter functions relative to (a) TOA solar flux and (b) NO_2 and O_3 absorption coefficients. One Dobson Unit (DU) equals 2.69×10^{16} molecules/cm^2.

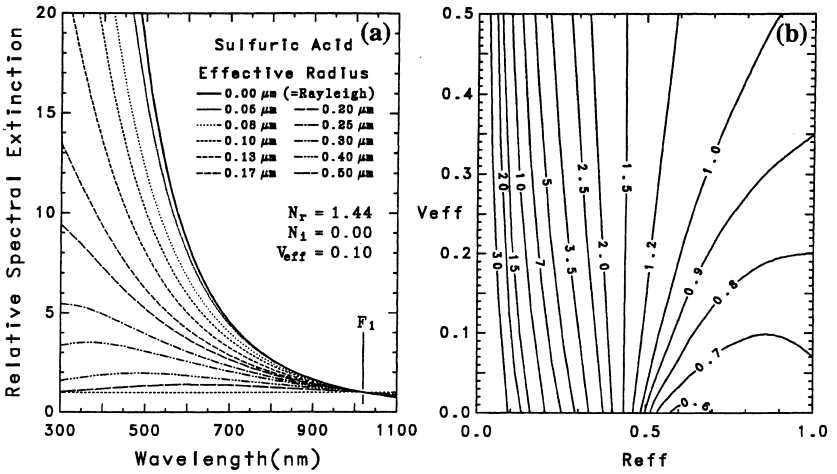

Fig. 4. Aerosol spectral extinction dependence on particle size for sulfuric acid. (a) spectral extinction relative to 1020 nm for effective variance $v_{\text{eff}} = 0.1$. (b) extinction ratio of 385–1020 nm for range of r_{eff} and v_{eff} used for obtaining initial aerosol size estimates.

sub-micron particles at visible wavelengths, the aerosol spectral extinction depends primarily on the aerosol size, with a significantly lesser dependence on the width (effective variance) of the size distribution which is shown in Fig. 4b.

In the present analysis, we use the standard gamma size distribution [12], and we assume a composition of concentrated sulfuric acid, appropriate for volcanic aerosols, with a refractive index of $m_r = 1.44, m_i = 0$ [18]. Choosing a different functional form for the size distribution would not noticeably affect the relative spectral extinction except possibly for very large variances. The dependence of aerosol spectral extinction on composition (refractive index) is also predictably regular, requiring only a rescaling of the retrieved particle sizes by the ratio of their respective real refractive index departures from unity [19].

Thus, we again emphasize that the relative spectral extinction of aerosols is rigorously constrained by Mie theory, albeit for specific values for r_{eff} and v_{eff} that are as yet, still to be determined, along with the aerosol optical depth and the ozone and NO_2 amounts. This implies the application of a brute force iterative least-squares search to find the best fit to the observed spectral extinction data.

A first guess estimate for the aerosol size, r_{eff}, at a particular altitude level, is provided by the ratio of the observed spectral extinction between the 385 nm and 1020 nm channels (by initially assuming no NO_2 absorption and by selecting a value for the variance, such as $v_{\text{eff}} = 0.1$ in Fig. 1a). This defines the aerosol spectral extinction at the other SAGE II channels for the specified r_{eff} and v_{eff}, and we are now in a position to perform a least-squares solution for δ_{ik}

in (8) to obtain the best spectral fit to the observed extinction at the ith tangent ray altitude. Using the retrieved aerosol optical depth (along with the prescribed r_{eff} and v_{eff}), and the retrieved ozone and NO_2 amounts in a forward calculation, we obtain the root-mean-square (RMS) difference between the modeled and observed spectral extinctions which serves as a quantitative measure in terms of which to describe the quality of the model fit to the observed spectral extinctions.

We apply the least-squares search over a coarse grid of r_{eff} and v_{eff} values, thus effectively searching the full extent of Fig. 1b, to locate the specific r_{eff} and v_{eff} mesh point that will minimize the RMS residuals to the observed spectral extinction. Because of the physical complexity of the data, local minima may exist, preventing application of more rapidly converging search techniques. As the iterative procedure continues, the grid size is reduced over the course of several iterations, thus locating the specific r_{eff} and v_{eff} values that, together with the least-squares determined aerosol optical depth and ozone and NO_2 amounts, constitute the best-fit physical model to the observed spectral extinctions.

We again stress the point that the same least-squares iterative search technique is applied independently at each altitude of the vertical-path extinction profile. Naturally, there is advantage to utilize neighboring layer retrieved parameters to initialize the least-squares search. As may be seen from Figs. 3 and 4, ozone and NO_2 contribute significant extinction in at least several of the SAGE II channels, while aerosols contribute extinction in all of the channels. Water vapor, however, absorbs only within the 940 nm channel, and because of this, does not participate fully in the least-squares fit. Thus water vapor is effectively retrieved as the left-over residual to the 940 nm aerosol extinction optical depth.

4. Retrieval results

Fig. 5a shows a sample atmospheric ozone profile retrieved from SAGE II slant-path spectral extinction data for a specific sunset occultation (Lat = 19.364, Lon = 99.764, Date = 85/01/17). Also shown in the figure (by the dashed curve) is the ozone profile obtained using the operational SAGE II inversion algorithm [6]. Overall, the agreement is seen to be excellent, with a slight off-set evident in retrieved profiles. Fig. 5b shows a similar comparison for NO_2. Once again, the overall agreement is quite good, but it is evident from the NO_2 profile that vertical smoothing is being used in the SAGE II algorithm. Data drop-outs occur in NO_2 amount at altitudes below $\approx$20 km when the least-squares fitting returns negative NO_2 amounts. This is not allowed. In such cases, the NO_2 amount is set to zero and the spectral extinctions are then refitted. This situation arises when the NO_2 extinction becomes small relative to

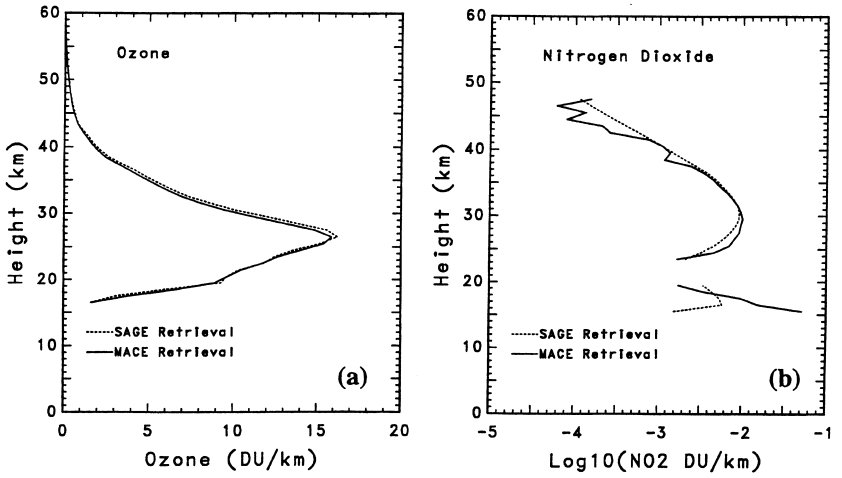

Fig. 5. Sample vertical profile retrievals obtained with MACE retrieval algorithm for atmospheric (a) ozone and (b) NO_2 profiles. Dashed lines depict SAGE operational algorithm results.

aerosol extinction, and when the aerosol spectral extinction itself becomes more complex (e.g., multi-modal) than can be spectrally represented by the mono-modal aerosol model used in the analysis. As a result, the retrieved NO_2 profiles appear to be reliable only above $\approx$20 km.

The retrieved aerosol optical depth and aerosol size parameters r_{eff} and v_{eff} are shown in Fig. 6 for the same SAGE II 85/01/17 sunset occultation. Fig. 6a

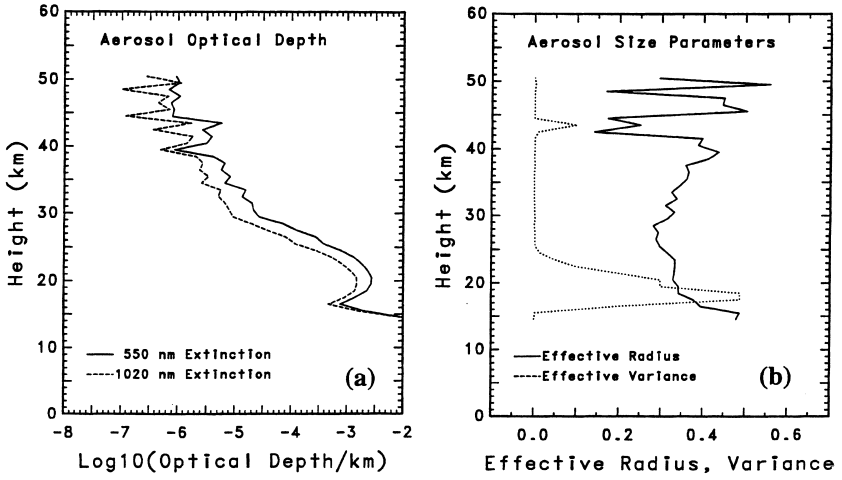

Fig. 6. Sample retrievals obtained with the MACE retrieval algorithm of (a) aerosol optical depth, shown at 550 and 1020 nm, and (b) aerosol size distribution parameters, r_{eff} and v_{eff}.

shows the height profile of aerosol extinction optical depth at 1020 nm, and also referenced at 550 nm. The reference optical depth at 550 nm is an inferred value from Mie scattering results, and is self-consistent and fully defined via the size parameters r_{eff} and v_{eff}. The 1020 nm optical depth, on the other hand, is very nearly the raw vertical-path extinction at 1020 nm, differing only by the small amount of O_3 absorption that is present in the 1020 nm channel, and by the small RMS residual at this wavelength due to the least-squares fitting.

Of note in Fig. 6b is the rather smooth vertical trend and layer-to-layer coherence of the retrieved size parameters r_{eff} and v_{eff}. Since retrievals at different heights are independent of each other, this suggests a physical basis for the inferred height dependence of the particle size and variance. The decrease in particle size with height (within the 20–25 km region) is expected and appears plausible. More questionable is the apparent decrease and small value of the size distribution variance, particularly in view of the multiple size modes that have been observed for stratospheric aerosols following the Pinatubo eruption [18]. Possibly, the time period of January 1985, that we have selected as the background level for the present study of the Nevado del Ruiz (November 1985) eruption, may represent quiescent conditions, being several years after the last major volcanic eruption of E1 Chichon in June 1983.

The apparent increase in particle size above ≈30 km (as the aerosol optical depth is decreasing to negligible values) raises more questions than it provides answers. In any case, rather than assigning literal physical reality to the retrieved size distribution parameters, we note only that the retrieved values, r_{eff} and v_{eff}, fit the observed spectral extinctions exceedingly well at the (sparsely spaced) SAGE II wavelengths. Broader variances (which the model is free to select) result in larger RMS errors. At altitudes above ≈40 km, the retrieved aerosol optical depths and size parameters become too noisy to be useful.

Fig. 7a shows the surface area density ($\mu m^2/cm^3$), a quantity that is relevant for atmospheric chemistry modeling. This is derived directly from the aerosol size and optical depth information for the same occultation event described above. The retrieved results are very similar to the surface area density climatology described by Thomason et al. [20].

Fig. 7b provides a quantitative measure of the quality of the retrieval model fit to the observed data. The profile of RMS error (expressed here as an optical depth/km) is plotted together with the 1020 nm channel aerosol optical depth/km. As may be seen the unexplained RMS residual of the least-squares fit is nearly two orders of magnitude smaller than the aerosol optical depth within the prime 20–25 km retrieval region. Further comparison must also be made to Fig. 2b which shows the 1020 nm channel vertical-path spectral extinction is much smaller than that in the other SAGE II channels. Thus, the unexplained spectral extinction RMS residual is remarkably small over the entire extent of the atmosphere. This serves to underscore the robustness of the MACE retrieval algorithm as applied to SAGE II occultation data.

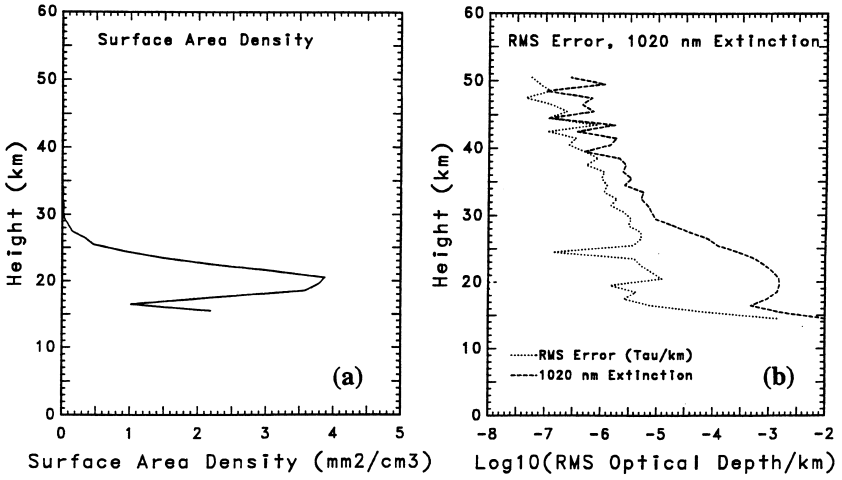

Fig. 7. Sample retrieval obtained with the MACE algorithm of (a) the aerosol surface area density, (b) RMS error of unexplained spectral extinction of the least-squares MACE analysis retrieval fits.

The SAGE II algorithm reports aerosol extinction at the 'aerosol' channel wavelengths of 385, 453, 525 and 1020 nm, but does not explicitly retrieve aerosol size distribution parameters. Here, again, comparisons shown in Fig. 8 of the SAGE retrieved extinction profiles with the equivalent MACE retrieval results shows excellent overall agreement (similar to that obtained for ozone and NO_2). However, a rigorous comparison is not easily accomplished because while the MACE retrieved aerosol spectral extinction represents a self-consistent physical model (via Mie scattering for the specified r_{eff} and v_{eff}), the SAGE retrieved spectral extinction represents a much more complicated aerosol model from which a unique aerosol size distribution can not be directly inferred. Also, vertical smoothing is evident in the SAGE retrievals, but is not used in the MACE results. Nevertheless, least-squares fits to the SAGE derived spectral extinctions do produce aerosol size variations that are close to the MACE retrievals, but the size distribution variance has to be assumed from other considerations, as we did to characterize Pinatubo volcanic aerosol size using SAGE II derived aerosol spectral optical depths and ISAMS extinction measurements at 12.1 μm [21].

Fig. 9 (top panel) shows the change in stratospheric aerosol mass due to the November 15, 1985 Nevado del Ruiz volcanic eruption in the form of a zonal mass anomaly plot (January 1986–January 1985), which is intended to remove the climatological stratospheric background. The zonally integrated aerosol mass is expressed in metric tons per 1 km × 1° latitude grid box (assuming for simplicity unit mass density for the aerosol). The changing spatial extent of the volcanic aerosol cloud provides a means to view the action of stratospheric

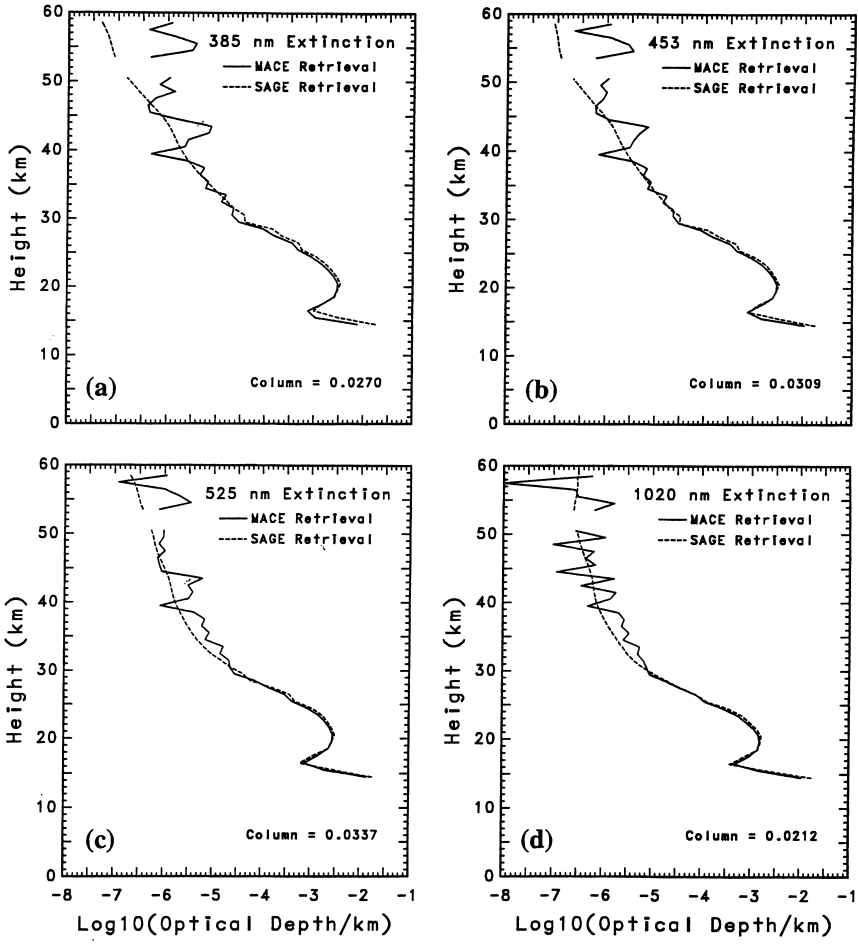

Fig. 8. Comparison of MACE retrieved aerosol spectral extinction profiles (solid lines) and SAGE II retrieval products (dashed lines) at 385, 453, 525, and 1020 nm, respectively.

dynamical transports. The negative mass numbers that are seen over most of the stratosphere between 20 and 30 km are indicative of the slow gravitational settling of the remnants of the E1 Chichon volcanic cloud during the course of a year. Notable in Fig. 9(top) is the strong confinement of the main Nevado del Ruiz aerosol cloud between latitudes −5°S and 12°N and between altitudes 20–25 km, with visible plumes of volcanic aerosol being wafted primarily northward (but also toward the south) at an altitude of about 30 km. The chaotic structure below 20 km is climatic noise in tropospheric aerosol variations.

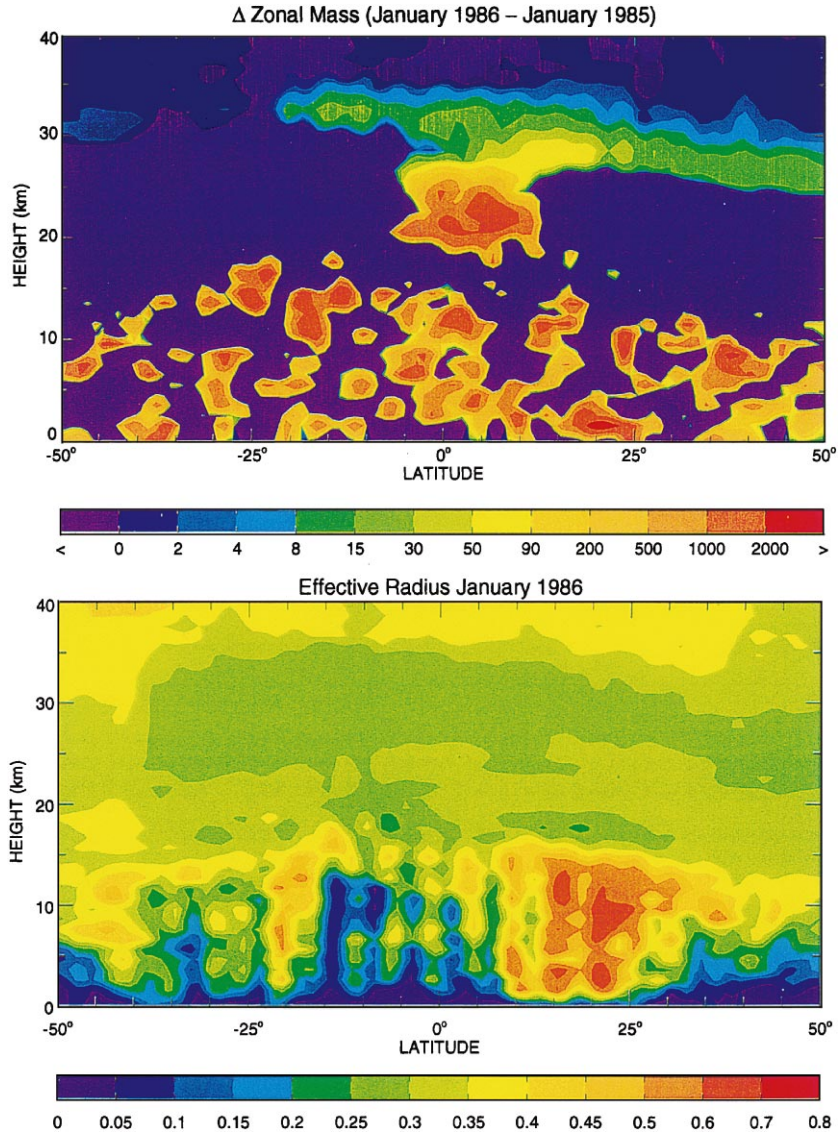

Fig. 9. Monthly-mean height-latitude maps of SAGE II zonal mass and effective radius variations. (top) Positive anomalies (January 1986–January 1985) of Nevado del Ruiz stratospheric aerosol mass (tons/km/deg Lat). (bottom) January 1986 stratospheric variation of aerosol effective radius (μm).

The bottom panel of Fig. 9 shows height variations of the stratospheric aerosol size distribution (effective radius) for January 1986. The stratospheric size distribution is characterized by a broad minimum in the 25–30 km region

with increasing sizes toward higher and lower altitudes. The general structure of the vertical distribution of aerosol size is similar to that shown in Fig. 6b. It is of interest that there is little change in the particle size distribution from the time before the eruption. If anything, there is an apparent decrease in particle size within the volcanic cloud region, indicative perhaps of the formation of a large number of small particles that drive down the mean particle size while increasing the optical depth of the aerosol cloud.

5. Discussion

The MACE retrieval algorithm is a physical model that utilizes accurately measured absorption coefficients for NO_2 and O_3, including their temperature dependence, to define the solar spectrum weighted SAGE II filter parameters in Eq. (9). Similarly the spectral extinction by aerosols is rigorously constrained by Mie theory for the specified refractive index and size distribution at the tabulated values of effective radius and variance. As already noted, we use the gamma size distribution for the aerosol size distribution. (Performing the same MACE retrieval analysis with a log normal size distribution would have produced the same results as obtained with the gamma distribution. Only for large variances there might be discernable differences.) However, particle number density, which is sensitive to the shape of the size distribution, will have significant dependence on the specific form of size distribution that is used. For completeness, we also performed the MACE retrieval using different aerosol compositions.

For conservative and near-conservative scattering aerosols, the retrieved aerosol sizes scale according to their refractive index ratios following van de Hulst [19], with negligible effect on the retrieved NO_2 and O_3 amounts. In the case of strongly absorbing aerosols, which have a different spectral extinction dependence, there are greater differences in the retrieved parameters, but since the RMS errors were also significantly larger, we discarded these results.

Overall, the MACE retrieved vertical profiles for ozone, NO_2, and aerosol optical depths agree closely with those obtained using the current (v5.931) SAGE algorithm [6]. As noted above, the retrieval differences, are probably due to the reverse order of species and geometric inversion, which imposes a different aerosol model on the retrieval analysis. Also, there is a difference in the way that retrieval uncertainties and modeling errors are displayed. In the MACE approach, with the simultaneous retrieval of all species, the RMS residuals quantitatively pass judgement on the goodness of the retrieval fit by the amount of unexplained spectral extinction. A similar quantity is not directly available from the SAGE retrieval, making it hard to critically compare the two retrieval approaches in detail. Instead, the SAGE results include as part of their retrieval uncertainty the effects of pressure–temperature profile

uncertainties on the amount of Rayleigh extinction, which is not included as a source of error in our analysis.

The main advantage of the MACE approach is that retrieval of all contributing constituents is simultaneous, thus minimizing the potential biases that might arise from having to assume a specific spectral dependence for interpolating aerosol extinction between different channels. While it is reassuring that the unexplained RMS residual in MACE retrievals is exceedingly small, real uncertainties remain. But these are largely attributable to the specific location and sparsity of the SAGE II filters. As a result, the limited spectral constraints that are imposed by the observational data on the retrieved solution may permit other combinations of aerosol size and gaseous absorbers to reproduce the observed spectral extinctions within observational error. Nevertheless, to be a contender, any other potential retrieval result must be able to fit the observed spectral extinctions with RMS errors that are at least as small as those obtained with the MACE algorithm. This retrieval validation problem can only be resolved by obtaining more complete spectral measurements which should happen with the advent of new SAGE III observations. The MACE retrieval algorithm is readily applicable to the analysis of SAGE III slant-path extinction data – all that is needed are the SAGE III filter functions to generate the appropriate filter parameters defined by Eq. (9).

The Nevado del Ruiz results in Fig. 9 provide the rationale for performing the MACE analysis retrieval on the SAGE II slant-path extinction data since this type of information is not available from the currently archived SAGE II data products. The intriguing feature is the strong confinement of the Nevado del Ruiz aerosol cloud to equatorial latitudes at altitudes below 30 km at $-5°$S latitude and 25 km at 12°N latitude. There is a plume of volcanic aerosol that is being carried northward (with a branch also going south) at an altitude of about 30 km. These results are surprising, given early indications based on TOMS measurements of emitted SO_2 that the Nevado del Ruiz eruption was mostly tropospheric [22], although the eruption cloud is clearly seen as a stratospheric feature in the SAGE II aerosol optical depth maps [20]. Apparently due to difficulty in tracking the SO_2 eruption plume, Krueger et al. [22], concluded that most of the estimated 6.6×10^5 tons of volcanic SO_2 was confined to the upper troposphere. From our MACE retrievals, we estimate the stratospheric loading of SO_2 (above 17 km) to be about 3×10^5 tons. This is based on the peak volcanic aerosol mass anomaly of 6×10^5 tons. This occurs in March 1986, 4 months after the 15 November 1985 Nevado del Ruiz eruption. For comparison, the January 1986 (Fig. 9(top)) SO_2 mass anomaly above 17 km is about 2×10^5 tons, implying a time scale of several months for the photochemical conversion of SO_2 to H_2SO_4.

The strong latitudinal confinement of the Nevado del Ruiz aerosol cloud to equatorial latitudes supports the "tropical pipe" model of stratospheric transport described by Plumb [23], whereby the tropical region of the strato-

sphere remains isolated from the isentropic stratospheric mixing occurring at middle latitudes. Likewise, the pole-ward directed plumes near the 30 km altitude in Fig. 8a trace out the meridional circulation of the tropical pipe model. As a practical example, the rate at which the lower stratospheric extra-tropical air mixes into the tropical pipe and is then lofted upward has direct impact on the extent to which midlatitude aircraft emissions will affect the ozone layer. Hall and Waugh [24] used HALOE measurements of stratospheric H_2O and CH_4 to infer the relevant stratospheric transport parameters. From this study, it is abundantly clear that the Nevado del Ruiz aerosol can serve as an excellent inert tracer of stratospheric dynamical transports. This has great potential to reduce the current uncertainty in the mixing time scales between the tropics and the midlatitudes.

6. Conclusions

A successful application of the MACE algorithm to analyze SAGE II slant-path extinction data has been amply demonstrated. The retrieved profiles of ozone, NO_2, and aerosol optical depth agree closely with the operational SAGE II algorithm retrievals. By performing simultaneous retrieval of all species, and by using a well defined physical model for aerosol spectral extinction, we minimize the potential for introducing unintended biases in the retrieved results. In the process, we obtain simultaneous retrieval of aerosol size information in the form of size distribution parameters r_{eff} and v_{eff}, which, together with the retrieved aerosol optical depth define the aerosol mass density. Knowing the size and mass density of the aerosol, and its time evolution, permits quantitative tracking of the aerosol gravitational settling and the inference of transport by stratospheric dynamics.

The data inversion model described here consists of two basic components. First, the geometric inversion of the slant-path extinction profiles, which can be performed independently of the species retrieval without introducing unnecessary assumptions, should be performed first as recommended by Rusch et al. [10], rather than following the procedure of the SAGE II algorithm [6]. We show that fast inversion of the slant-path extinction profiles can be accomplished with a simple geometric algorithm without imposing significant physical assumptions. Subtracting out the Rayleigh scattering contribution is accomplished with high precision to obtain the vertical-path non-Rayleigh spectral extinction that serves as data input for the species retrieval component of the current inversion scheme.

We minimize the introduction of retrieval bias by performing a simultaneous least-squares species inversion using the best physical models for the spectral extinction dependence of each contributor. In this respect, the MACE retrieval algorithm that we developed for analyzing ground-based MFRSR

measurements has proven to be a versatile retrieval tool as demonstrated by its ability to analyze a totally different data set with different spectral data input without requiring any significant change in operational procedure.

The results of this study show that the SAGE II observational data contain a great deal of valuable information that as yet has not been fully exploited. Specifically, the results show great potential for tracking stratospheric dynamics by using the del Ruiz aerosol as an inert tracer of stratospheric dynamics. Further, a detailed mapping of the stratospheric aerosol size and optical depth information should serve to reduce the current uncertainties in the mixing rate time scales of stratospheric transports. With the advent of higher spectral resolution and greater measurement frequency of SAGE III observations, more detailed and better constrained retrievals will be possible.

Acknowledgements

This work was supported in part by the NASA Atmospheric Chemistry Modeling and Analysis Program, by the NASA Radiation Science Program and by the Department of Energy Atmospheric Radiation Measurement (ARM) Program. We also thank Larry Thomason for providing the SAGE II data for the Ruiz volcanic eruption period. The authors Lacis and Hansen gratefully acknowledge Prof. S. Ueno's hospitality and encouragement when they were graduate students at the University of Kyoto.

References

[1] J.E. Hansen, S. Matsushima, Light illuminance and color in the earths shadow, J. Geophys. Res. 71 (1966) 1073–1081.
[2] F. Link, Eclipse Phenomena, Springer, Berlin, 1969.
[3] L.E. Mauldin III, N.H. Zaun, M.P. McCormick, J.H. Guy, W.R. Vaughn, Stratospheric Aerosol and Gas Experiment II instrument: a functional description, Opt. Eng. 24 (1985) 307–312.
[4] W.P. Chu, M.P. McCormick, Inversion of stratospheric aerosol and gaseous constituents from solar extinction data in the 0.38–1.0 μm wavelength region, Apl. Opt. 18 (1979) 1404–1413.
[5] W.P. Chu, Calculations of atmospheric refraction for spacecraft remote sensing applications, Apl. Opt. 22 (1983) 721–725.
[6] W.P. Chu, M.P. McCormick, J. Lenoble, C. Brogniez, P. Pruvost, SAGE II inversion algorithm, J. Geophys. Res. 94 (1989) 8339–8351.
[7] H.M. Steele, R.P. Turco, Separation of aerosol and gas components in the Halogen Occultation Experiment and the Stratospheric Aerosol and Gas Experiment (SAGE) II extinction measurements: Implications for SAGE II ozone concentration trends, J. Geophys. Res. 102 (1997) 19665–19681.
[8] D. Fussen, Critical analysis of the Stratospheric Aerosol and Gas Experiment II spectral inversion algorithm, J. Geophys. Res. 103 (1998) 8455–8464.
[9] S. Twomey, Introduction to the mathematics of inversion in remote sensing and indirect measurements, in: Developments in Geomathematics, Elsevier, New York, 1977.

[10] D.W. Rusch, C.E. Randall, M.T. Callan, M. Horanyi, R.T. Clancy, S.C. Solomon, S.J. Oltmans, B.J. Johnson, U. Koehler, H. Claude, D. De Muer, A new inversion for Stratospheric Aerosol and Gas Experiment II data, J. Geophys. Res. 103 (1998) 8465–8475.
[11] C.W. Allen, Astrophysical Quantities, The Athlone Press, London, 1973.
[12] J.E. Hansen, L.D. Travis, Light scattering in planetary atmospheres, Space Sci. Rev. 16 (1974) 527–610.
[13] A.T. Young, Revised depolarization correction for atmospheric extinction, Apl. Opt. 19 (1980) 3427–3428.
[14] A.A. Lacis, B.E. Carlson, B. Cairns, Multi-spectral atmospheric column extinction analysis of multi-filter rotating shadowband radiometer measurements, in: Proceedings of the Sixth Atmospheric Radiation Measurement (ARM) Science Team Meeting, San Antonio, TX, 1997, pp. 145–148.
[15] J.W. Harder, J.W. Brault, P.V. Johnston, G.H. Mount, Temperature dependent NO_2 cross sections at spectral resolution, J. Geophys. Res. 102 (1997) 3861–3879.
[16] M.F. Merienne, A. Jenouvrier, B. Coquart, The NO_2 absorption spectrum I: absorption cross-sections at ambient temperature in the 300–500 nm region, J. Atmos. Chem. 20 (1995) 281–297.
[17] W. Schneider, G.K. Moortgat, G.S. Tyndall, J.P. Burrows, Absorption cross-sections of NO_2 in the uv and visible region (200–700 nm) at 298 K, J. Photochem. and Photobio A: Chem. 40 (1987) 195–217.
[18] T. Deshler, B.J. Johnson, W.R. Rozier, Balloonborne measurements of Pinatubo aerosol during 1991 at 41°N, vertical profiles, size distribution, and volatility, Geophys. Res. Lett. 20 (1993) 1435–1438.
[19] H.C. van De Hulst, Light Scattering by Small Particles, Wiley, New York, 1957.
[20] L.W. Thomason, L.R. Poole, T. Deshler, A global climatology of stratospheric aerosol surface area density deduced from Stratospheric Aerosol and Gas Experiment II measurements: 1984–1994, J. Geophys. Res. 102 (1997) 8967–8976.
[21] A.A. Lacis, B.E. Carlson, B. Cairns, Multi-spectral atmospheric column extinction analysis of multi-filter rotating shadowband radiometer measurements, in: Proceedings of the Sixth Atmospheric Radiation Measurement (ARM) Science Team Meeting, San Antonio, TX, 1997, pp. 145–148.
[22] A.J. Krueger, L.S. Walter, C.C. Schnetzler, S.D. Doiron, Toms measurement of the sulfur dioxide emitted during the 1985 Nevado del Ruiz eruptions, J. Volcanology Geothermal Res. 41 (1990) 7–15.
[23] R.A. Plumb, A tropical pipe model of stratospheric transport, J. Geophys. Res. 101 (1996) 3957–3972.
[24] T.M. Hall, D. Waugh, Tracer transport in the tropical stratosphere due to vertical diffusion and horizontal mixing, Geophys. Res. Lett. 24 (1997) 1383–1386.